

Primljen / Received: 6.3.2019.

Ispravljen / Corrected: 2.6.2019.

Prihvaćen / Accepted: 22.9.2019.

Dostupno online / Available online: 10.10.2020.

Analysis of model helical piles subjected to axial compression

Authors:



Yakup Türedi, MCE

Iskenderun Technical University, Turkey
Faculty of Engineering and Natural Sciences
Civil Engineering Department
yakup.turedi@iste.edu.tr



Prof. **Murat Örnek**, PhD. CE

Iskenderun Technical University, Turkey
Faculty of Engineering and Natural Sciences
Civil Engineering Department
murat.ornek@iste.edu.tr

Corresponding author

Research Paper

Yakup Türedi, Murat Örnek

Analysis of model helical piles subjected to axial compression

An investigation into axial compression capacity of single helical piles placed in dry sand through laboratory model tests and numerical analyses is presented. The compressive bearing capacities were compared with existing theoretical results given in the literature. Laboratory model tests were performed to determine some design parameters of helical piles such as the plate number, plate diameter, and plate spacing. A good correspondence between experimental, numerical, and theoretical results was established.

Key words:

helical pile, compression, model test, numerical analyses, sand

Prethodno priopćenje

Yakup Türedi, Murat Örnek

Analiza osnotlačno opterećenih modela spiralnih pilota

U radu je prikazano istraživanje otpornosti pojedinačnih osnotlačno opterećenih spiralnih pilota u suhom pijesku pomoću laboratorijskih fizikalnih modela i numeričkih analiza. Dobivene vrijednosti tlačne nosivosti uspoređene su s postojećim teoretskim rezultatima iz literature. Laboratorijska ispitivanja na modelima provedena su kako bi se odredili neki od parametara potrebnih za projektiranje spiralnih pilota, kao što su broj, promjer i razmak spiralnih ploča. Rezultati su pokazali da broj, veličina i razmak spiralnih ploča utječu na ponašanje spiralnih pilota. Utvrđena je dobra podudarnost između eksperimentalnih, numeričkih i teoretskih rezultata.

Ključne riječi:

spiralni pilot, tlak, modelsko ispitivanje, numeričke analize, pijesak

Vorherige Mitteilung

Yakup Türedi, Murat Örnek

Analyse axial belasteter Spiralpfahlmodelle

Die Arbeit präsentiert eine Studie über den Widerstand einzelner axial belasteter Spiralpfähle in trockenem Sand unter Verwendung physikalischer Labormodelle und numerischer Analysen. Die erhaltenen Werte der Druckkapazität wurden mit den vorhandenen theoretischen Ergebnissen aus der Literatur verglichen. Labortests an den Modellen wurden durchgeführt, um einige der Parameter zu bestimmen, die für die Planung von Spiralpfählen erforderlich sind, wie z. B. Anzahl, Durchmesser und Abstand der Spiralplatten. Die Ergebnisse zeigten, dass Anzahl, Größe und Abstand der Spiralplatten das Verhalten der Spiralpfähle beeinflussen. Es wurde eine gute Übereinstimmung zwischen experimentellen, numerischen und theoretischen Ergebnissen gefunden.

Schlüsselwörter:

Spiralpfahl, Druck, Modellprüfung, numerische Analyse, Sand

1. Introduction

As known, deep foundations are preferred if geotechnical requirements can not be met by shallow foundations. One type of deep foundations, called helical piles (known as torque driven piles), has been widely used in engineering applications and in many countries because of their numerous advantages. Some of these advantages are:

- installation under variable weather and site conditions
- cost effectiveness and fast installation
- easy transportation, removal, and reuse
- immediate load carrying capability
- easy construction in various soil conditions
- instant use
- advantages over the traditional pile system, i.e. installation with traditional equipment.

Moreover, they can provide structural stability in uplift tension, axial compression, lateral force, and overturning moment for static and dynamic loads. This type of piles, i.e. helical piles, are currently used in many civil engineering applications such as residential and commercial buildings, bridges, foundations of damaged buildings and risk-prone buildings, foundations of historical buildings, foundations of energy systems such as wind turbines and solar panels, light poles, machine foundations, pipelines, transmission tower foundations, pier supports, marine anchors and braced excavations. The installation of helical pile foundations is a vibration-free process (so it is appropriate in foundation reinforcing applications of sensitive structures) and there is no pulp material during installation of helical piles. Due to these properties, helical piles are considered environmentally friendly [1-3].

In this study, the behaviour of the axial compressive loaded model helical piles in sand soil is determined using small-scale model tests and finite element based numerical analyses. The effects of the helical plates number (single and double), helical plate spacing ratio (s/D) (1, 1.5, 2, 2.5 and 3) and helical plate diameter (50 mm, 75 mm, 100 mm, and 125 mm) on the compression bearing capacity are investigated. The model test results are compared with theoretical results given in the literature. Good correspondence was observed between test, numerical, and theoretical results.

2. Literature review

Helical piles have become a subject of growing interest in recent decades. When the amount of available research and design methods are examined, the compression behaviour of helical piles is more limited than other conventional pile foundation and tension conditions [4].

Sakr [5] performed a series of tension and compression tests

using large capacity single and double-helix piles in soils of varying densities. Out of eleven experiments, seven were pressure tests and four were tensile tests. As a consequence, individual bearing method is preferred to estimate the ultimate capacity of piles. The general behaviour is affected by pile geometry, groundwater characteristics, soil profile, and installation procedures. Also, axially loaded helical piles have revealed significant compressive resistance of up to approximately 1920 kN. Malik et al. [6] investigated the bearing capacity of pipe pile and screw pile by means of small scale loading tests. The load and settlement curve is affected by pile tip diameter, both for pipe pile and screw pile. Li and Deng [7] researched the axial load of different types of single helical piles of small diameter. A couple of helical piles were installed in granular and cohesive soil, and subjected to load. These authors concluded that behaviour of helical piles can accurately be estimated by hyperbolic approach. After these tests, some parametric studies were performed to define an optimum equivalent shaft length. Numerical investigations have also been conducted about the axial compression behaviour of helical piles, as can for instance be seen in [4, 8-10]. Full-scale loading tests and numerical analyses were performed by Livneh and Naggar [4] in order to investigate axial compression performance of helical piles. These authors established that cylindrical shear failure is dominant in the load transfer mechanism. Sprince and Pakrastinsh [8] examined compression behaviour of the helical piles system using three calculation methods and the finite element calculation simulation in four different soils. They established that the capacity enlarged with enlargement of the helical plate. Salhi et al. [9] investigated behaviour of helical piles in cohesionless soils and the effect of the spacing ratio (s/D_h) (s refers helix spacing and D_h refers helix diameter) by the two dimensional finite element approach compared with large-scale test results. They concluded that mechanism of load transfer from cylindrical shear failure to individual bearing failure changes when the spacing ratio (s/D_h) is changed from 1.5 to 2. Polishchuk and Maksimov [10] investigated full-scale helical pile field tests results in clay soils using the finite element analysis. They reported that model results are in accordance with test results.

3. Methods for estimating bearing capacity

Several design methods have been developed in the literature to define the axial bearing capacity of helical piles [11]. These methods are the cylindrical shear model and the individual bearing model (Figure 1). The cylindrical shear failure is observed in failure surface that connects the top and bottom helixes [4, 12-15]. The individual bearing method failure mechanism is characterized as the sum of all individual helical pile capacities along with the shaft resistance [4, 5, 13-18].

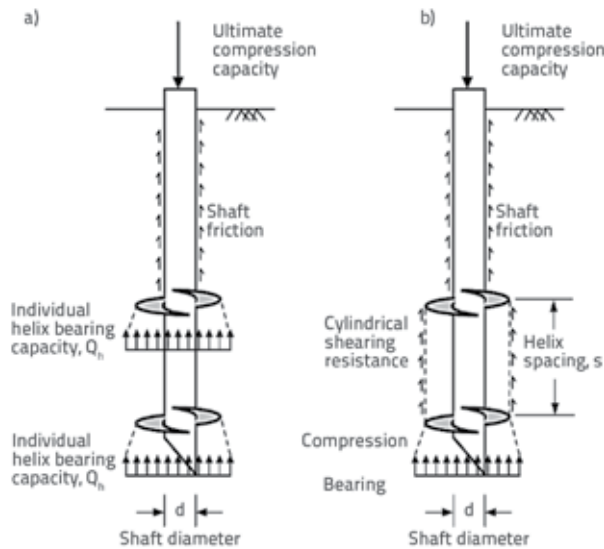


Figure 1. Estimation of helical pile behaviour under compression: a) individual bearing method; b) cylindrical shear method [14]

For granular soil, the ultimate compressive capacity of helical piles is determined by some formulas, as indicated below:

a) Cylindrical shearing method

$$Q_c = Q_{helix} + Q_{bearing} + Q_{shaft} \quad (1)$$

$$Q_{helix} = \frac{1}{2} \pi D_a \gamma' (H_b^2 - H_t^2) K_s \tan \varphi \quad (2)$$

$$Q_n = A_n q N_q \quad (3)$$

$$Q_{shaft} = \frac{1}{2} P_s H_{eff}^2 \gamma' K_s \tan \varphi \quad (4)$$

$$Q_c = \frac{1}{2} \pi D_a \gamma' (H_b^2 - H_t^2) K_s \tan \varphi + \gamma' H A_n N_q + \frac{1}{2} P_s H_{eff}^2 \gamma' K_s \tan \varphi \quad (5)$$

where:

- Q_c – ultimate compression capacity [kN]
- K_s – dimensionless coefficient of lateral earth pressure
- φ – internal friction angle [°]
- γ' – effective unit weight [kN/m³]
- A_n – net area of the undermost helix [m²]
- D_a – average helix diameter [m]
- N_q – dimensionless bearing-capacity factor
- H – embedment depth of pile [m]
- H_{eff} – effective shaft length [m]
- P_s – shaft perimeter [m]
- H_b – depth to undermost helix [m]
- H_t – depth to top helix [m].

b) Individual bearing method

$$Q_c = \gamma' H_b A_n N_q + \gamma' H_t A_t N_q + P_s H_{eff}^2 \gamma' K_s \tan \varphi \quad (6)$$

where:

- Q_c – ultimate compression capacity [kN]
- A_t – net surface area of the uppermost helix calculated from $(D^2 - d^2)/4$.

4. Materials and method

The experimental load tests were performed at Iskenderun Technical University, Geotechnical Laboratory of Civil Engineering Department, Hatay, Turkey. In total, thirty laboratory model tests were conducted for different diameters of helical plates (increase from 50 mm to 125 mm by 25 mm) and spacing ratios s/D from 1 to 3 in loose sand conditions. The experimental setup is given in Figure 2 and Figure 3.

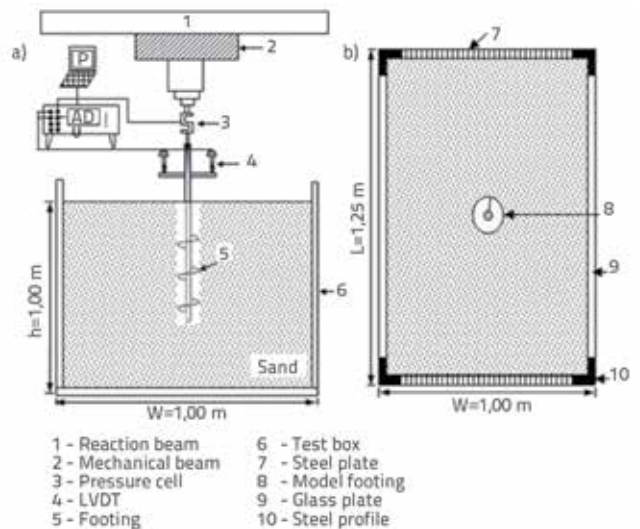


Figure 2. General views of test setup: a) elevation; b) plan



Figure 3. Test setup: overview

4.1. Test box

The model tests were performed using the following test box dimensions: 1.25 m x 1.0 m in plan and 1.0 m in depth.

Vertical and bottom sides of the box were strengthened to prevent lateral deformation during the soil filling and loading process. Two opposite side of the box are 10 mm in thickness, and are made of glass. The other sides measure 3 mm in thickness and are made of steel. In addition, four corners of the box rest on four steel columns. During the tests, the boundary distances of the test box were greater than the footing dimensions.

The loading system consists of an electrically operated mechanical jack and the load was vertically applied to helical footings of the model, with the loading frame mounted on the test box. The load-settlement measurements were conducted with a load cell and LVDTs (linear variable differential transformers). These LVDTs are accurate to 0.001 mm. They are placed between the model footing and the jack (Figure 2).

4.2. Sand soil

In order to describe the helical pile compression capacities, river sand (uniform, clean, fine) obtained from the Ceyhan River was used for model tests. Laboratory tests were conducted to determine strength parameters, maximum and minimum densities, specific gravity, and gradation of representative sand samples. These properties are tabulated in Table 1. Grain size distribution of the sand is shown in Figure 4. This sand was categorized using the USCS (Unified Soil Classification System) and marked as SP (poorly-graded sand). The measured internal friction angle determined for sand soil by conventional direct shear test amounted to 38°.

Table 1. Engineering properties of sand

Parameter	Value
Fraction of coarse sand [%]	0.00
Fraction of medium sand [%]	65.00
Fraction of fine sand [%]	35.00
D_{10} [mm]	0.18
D_{30} [mm]	0.28
D_{60} [mm]	0.58
Coefficient of uniformity, C_u	4.46
Coefficient of curvature, C_c	1.04
Specific gravity	2.75
Dry unit weight (dense sand) [kN/m ³], max.	17.11
Dry unit weight (loose sand) [kN/m ³], min.	15.44
Dry unit weight in model tests ($D_r = 25\%$) [kN/m ³]	15.84
Cohesion, c [kPa]	0.00
Classification (USCS)	SP

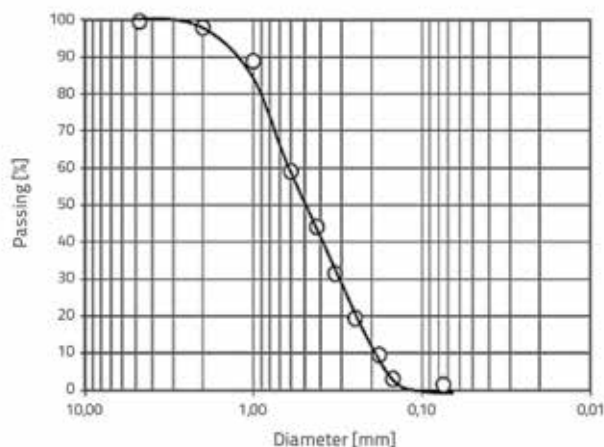


Figure 4. Grading curve of sand

4.3. Test plan

The loading test was conducted using a mild steel made rigid model helical pile plate. All model plates were 3 mm in thickness, and the steel pile shaft was 12 mm in diameter. Configurations of helical piles for evaluating the effect of increase in helical diameter and spacing ratio (s/D) on the compression ultimate load carrying capacity are summarized in Table 2. In the notation, HP refers to “helical pile”. Schematic view of the model helical pile is given in Figure 5, while geometric information is listed in Table 2.

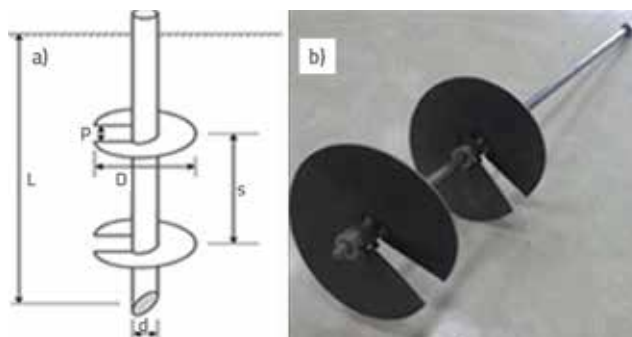


Figure 5. a) Schematic view of helical pile, b) model helical pile overview

In the tests, the sand soil was carefully placed at every 0.05 m up to top level of the test box. The maximum and minimum dry unit weights of the sand are 17.11 kN/m³ and 15.44 kN/m³, respectively (Table 1). In the tests, the test box was filled with sand, whose dry unit weight amounted to 15.84 kN/m³. In other words, the loose sand soil condition corresponding to about 25 % of relative density was considered. The model helical pile was installed by applying rotational force at the pile using a mechanical jack. The loading rate in the tests was 3.5 mm/min and the load was applied continuously. Loads and settlement relations for piles were measured with two LVDT’s placed on either side of the pile and load cell, as shown in Figure 2. Calibration was also

Table 2. Details of model tests

Test number	Pile name	Shaft		Helix plate		s/D	
		Length L [mm]	Diameter d [mm]	Diameter D [mm]	Thickness e [mm]	No of helixes	Spacing ratio
HP1	HP50	700	12	50	3	1	0.0
HP2		700	12	50	3	2	1.0
HP3		700	12	50	3	2	1.5
HP4		700	12	50	3	2	2.0
HP5		700	12	50	3	2	2.5
HP6		700	12	50	3	2	3.0
HP7	HP75	700	12	75	3	1	0.0
HP8		700	12	75	3	2	1.0
HP9		700	12	75	3	2	1.5
HP10		700	12	75	3	2	2.0
HP11		700	12	75	3	2	2.5
HP12		700	12	75	3	2	3.0
HP13	HP100	700	12	100	3	1	0.0
HP14		700	12	100	3	2	1.0
HP15		700	12	100	3	2	1.5
HP16		700	12	100	3	2	2.0
HP17		700	12	100	3	2	2.5
HP18		700	12	100	3	2	3.0
HP19	HP125	700	12	125	3	1	0.0
HP20		700	12	125	3	2	1.0
HP21		700	12	125	3	2	1.5
HP22		700	12	125	3	2	2.0
HP23		700	12	125	3	2	2.5
HP24		700	12	125	3	2	3.0

made before the model tests. The load-settlement readings were collected for each test using a data logger unit consisting of sixteen-channels (MM700 Series Autonomous Data Acquisition Unit). After this process, test data were converted using the Geotechnical Software-DS7. The tests were considered finished when failure occurred. That means that the testing ended when the load capacity of the jack was reached, or when an acceptable vertical displacement of helical pile was obtained. The test box was emptied after each test and refilled for the next one to keep conditions stable throughout the testing.

5. Test results and discussions

There are many methods involving failure criteria that are used for interpreting axial compression capacities obtained from load tests for helical pile foundations [4, 5, 9]. Some of these methods given in the literature are the L1-L2 method, Davisson criterion, slope-tangent method, ISSMFE criterion, BS 8004 criterion, FHWA criterion, and FDOT criterion as tabulated in Table 3:

Sakr [14] classified ultimate load calculations of the helical piles subjected to axial compression as given in Figure 6. According to Sakr [14], the failure load of a helical pile corresponds to the displacement of 5 % of the helix diameter. Since the loads corresponding to a 10 % displacement of the diameter of large sized helical piles will be relatively large, the 5 % criterion provides, for many cases, acceptable values for permissible vertical displacements.

Table 3. Failure criteria for helical piles

Failure criterion	Displacement at failure
L1-L2 Method	
Davisson's criterion [22]	PL/AE+ (D/120+4) [mm]
Slope-tangent method [23]	Defined as the deflection at the tangents intersection to the plunging failure section and the linear-elastic section*
ISSMFE criterion [24] and BS 8004 criterion	10 %D
FHWA criterion [25]	5 %D
FDOT criterion [26]	PL/AE + D/30 (when D > 0.61 m)

* Plunging section slope=14.3 mm/100 kN

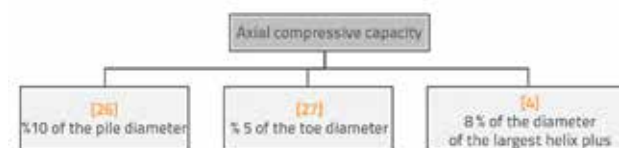


Figure 6. Ultimate compressive bearing capacities discussed in [14]

Another commonly used method is the Davisson's criterion [22] for the analysis of ultimate values of axially loaded helical piles (Figure 7). The ultimate load capacity directly depends on the total displacement, i.e. the sum of the elastic deflections of the pile and the offset, as shown in Equation 7 [4]:

$$S = \frac{PL}{AE} + \frac{D}{120} 4 \text{ [mm]} \tag{7}$$

where:

- S – displacement [mm]
- P – load on pile
- L – pile length [m]
- A – cross sectional area of the pile shaft
- E – Young’s modulus of pile material
- D – diameter of the largest helix [mm].

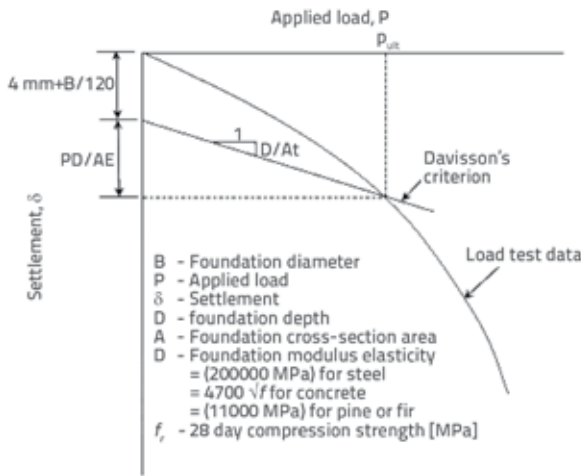


Figure 7. Davisson's criterion method

The effects of helix diameter and spacing ratio (s/D) of multi-helix helical piles under axial compression in sand soil were investigated by means of model tests. A total of 24 model tests were performed with four different helix diameters and five different spacing ratios. The load-displacement curves are presented in Figure 8. When the helix diameter size and spacing ratio increases the ultimate load also increases for all helical piles. The ultimate capacity in axial compression for all model helical piles is calculated using the individual bearing method and the cylindrical shear method. Table 5 presents the ultimate capacity results using equations (1) through (5) and failure criterion estimations. In the model tests, the 5 %, 10 % and Davisson's failure criteria were used for the estimation of ultimate compression capacities of helical piles. The prediction ratio (equation capacity/ failure criterion estimation) was used to find the best fit with the tests results. As can be seen in Table 5, the estimated capacities were in reasonable agreement with the capacities based on the 5 % of failure criterion. When the prediction ratio from this table is investigated, it can be concluded that the transition from the cylindrical shear failure phase to the individual bearing failure phase is observed when the spacing ratio ranges from 1.5 to 2.0. Spacing ratios in transition increase with an increase in helical diameter. Double helix piles exhibit approximately 90 to 100 % more resistance compared to single helix piles. Additionally, a non-linear relationship was found between the helical diameter and ultimate load. Table 5 presents proportional percentage

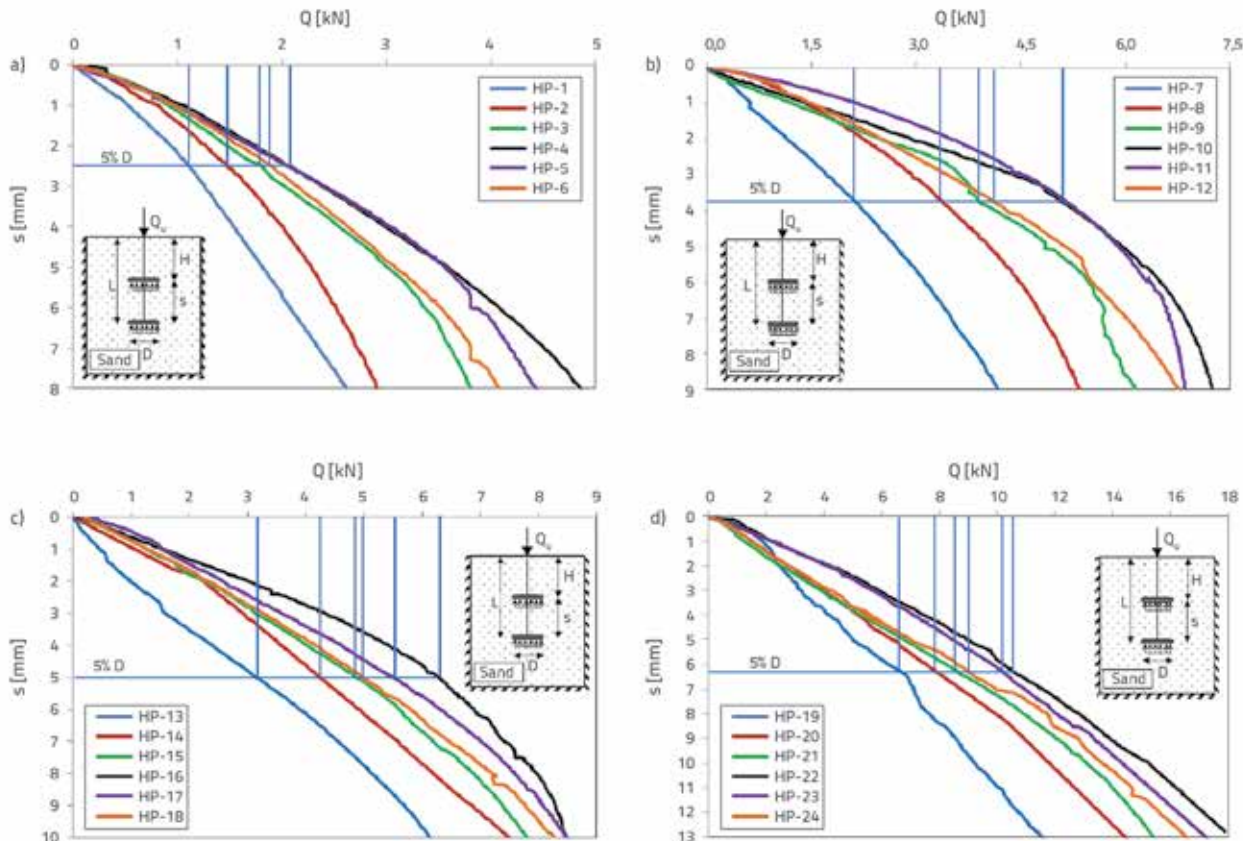


Figure 8. Axial compressive load test results: a) HP50; b) HP75; c) HP100; d) HP125, (HP - helical pile)

Table 4. Summary of axial compressive loads of helical piles in sand

Pile No.	No. of helixes	D [mm]	s/D	Measured capacity [kN]			Calculated capacity					Prediction ratio	
				5 %D	10 %D	Davisson method	The individual bearing method			Qu [kN]	The cylindrical shear method	5 %D	
							The element contributions [%]					The individual method	The cylindrical method
				Shaft	Helix	Bearing	Qu [kN]	Qu [kN]	The individual method	The cylindrical method			
HP-1	Single	50	0	1.15	1.70	1.66	2.31	97.69	0.00	1.07	1.07	0.93	0.93
HP-2	Double		1	1.40	2.25	2.12	1.17	57.55	41.29	1.82	1.10	1.30	0.78
HP-3	Double		1.5	1.73	2.95	2.72	1.09	58.56	40.35	1.79	1.11	1.03	0.64
HP-4	Double		2	2.10	3.51	3.26	1.02	59.61	39.37	1.76	1.12	0.84	0.53
HP-5	Double		2.5	2.15	3.50	3.28	0.95	60.69	38.36	1.72	1.13	0.80	0.53
HP-6	Double		3	1.90	3.15	2.88	0.89	61.81	37.31	1.69	1.14	0.89	0.60
HP-7	Single	75	0	2.15	3.70	2.60	1.04	98.96	0.00	2.38	2.38	1.11	1.11
HP-8	Double		1	3.35	5.95	3.80	0.47	56.77	42.75	4.15	2.44	1.24	0.73
HP-9	Double		1.5	3.80	5.70	4.70	0.43	58.35	41.22	4.03	2.47	1.06	0.65
HP-10	Double		2	4.90	6.75	5.75	0.38	60.02	39.60	3.92	2.49	0.80	0.51
HP-11	Double		2.5	5.00	6.70	5.80	0.34	61.78	37.88	3.81	2.51	0.76	0.50
HP-12	Double		3	4.20	6.20	5.00	0.30	63.65	36.05	3.70	2.54	0.88	0.60
HP-13	Single	100	0	3.15	6.10	3.10	0.59	99.41	0.00	4.21	4.21	1.34	1.34
HP-14	Double		1	4.25	7.20	4.25	0.24	56.88	42.87	7.36	4.32	1.73	1.02
HP-15	Double		1.5	4.65	7.70	4.80	0.21	59.09	40.70	7.08	4.36	1.52	0.94
HP-16	Double		2	5.60	8.30	5.40	0.18	61.48	38.34	6.81	4.40	1.22	0.79
HP-17	Double		2.5	6.30	8.32	6.30	0.15	64.06	35.79	6.53	4.44	1.04	0.71
HP-18	Double		3	5.30	8.20	5.20	0.12	66.86	33.01	6.26	4.48	1.18	0.84
HP-19	Single	125	0	6.60	11.10	5.20	0.38	99.62	0.00	6.56	6.57	0.99	0.99
HP-20	Double		1	7.83	14.00	6.30	0.14	57.40	42.46	11.39	6.73	1.46	0.86
HP-21	Double		1.5	8.10	15.00	6.90	0.12	60.30	39.58	10.84	6.80	1.34	0.84
HP-22	Double		2	10.53	16.50	8.60	0.10	63.51	36.40	10.30	6.86	0.98	0.65
HP-23	Double		2.5	10.14	17.70	9.00	0.07	67.07	32.85	9.75	6.91	0.96	0.68
HP-24	Double		3	9.20	16.00	7.50	0.05	71.06	28.89	9.20	6.96	1.00	0.76

of load amounts carried by pile elements according to the discrete transport method. It can clearly be seen that the load carried by helix increases with an increase in helical diameter and s/D ratio. While the ultimate compressive load for HP50 is 2.10 kN, this value increases to 5.60 kN for HP100 for a constant ratio of s/D = 2.

6. Finite element analyses

The compression behaviour of helical piles resting on sand soil bed is simulated by the finite element model using Plaxis 2D software [19]. It has been specially improved for the stability and deformation analysis in geotechnical engineering [20]. In this model, boundaries are free in vertical directions, while horizontal directions are constrained. Also, the bottom boundary is fully fixed: The 15-node triangular elements are used for modelling the soil environment. The analyses were performed using an axisymmetric condition model for helical plates in sand soil. A typical mesh distribution including soil and helical pile is given in Figure 9. Plaxis includes a lot of advanced material models with specific features. Out of these models, the elastic-plastic Mohr Coulomb (MC) model, covering the first order approximation of soil or rock, was chosen to simulate

sand behaviour. The MC model needs a small set of parameters to simulate soil behaviour in reality.

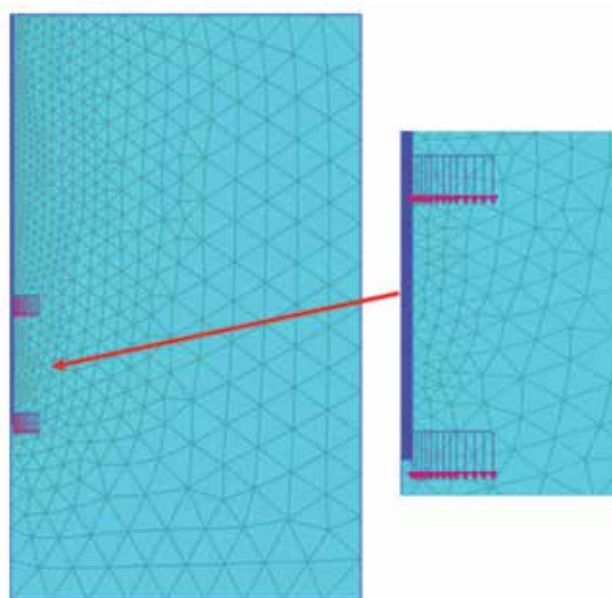


Figure 9. Typical mesh distribution obtained in the model

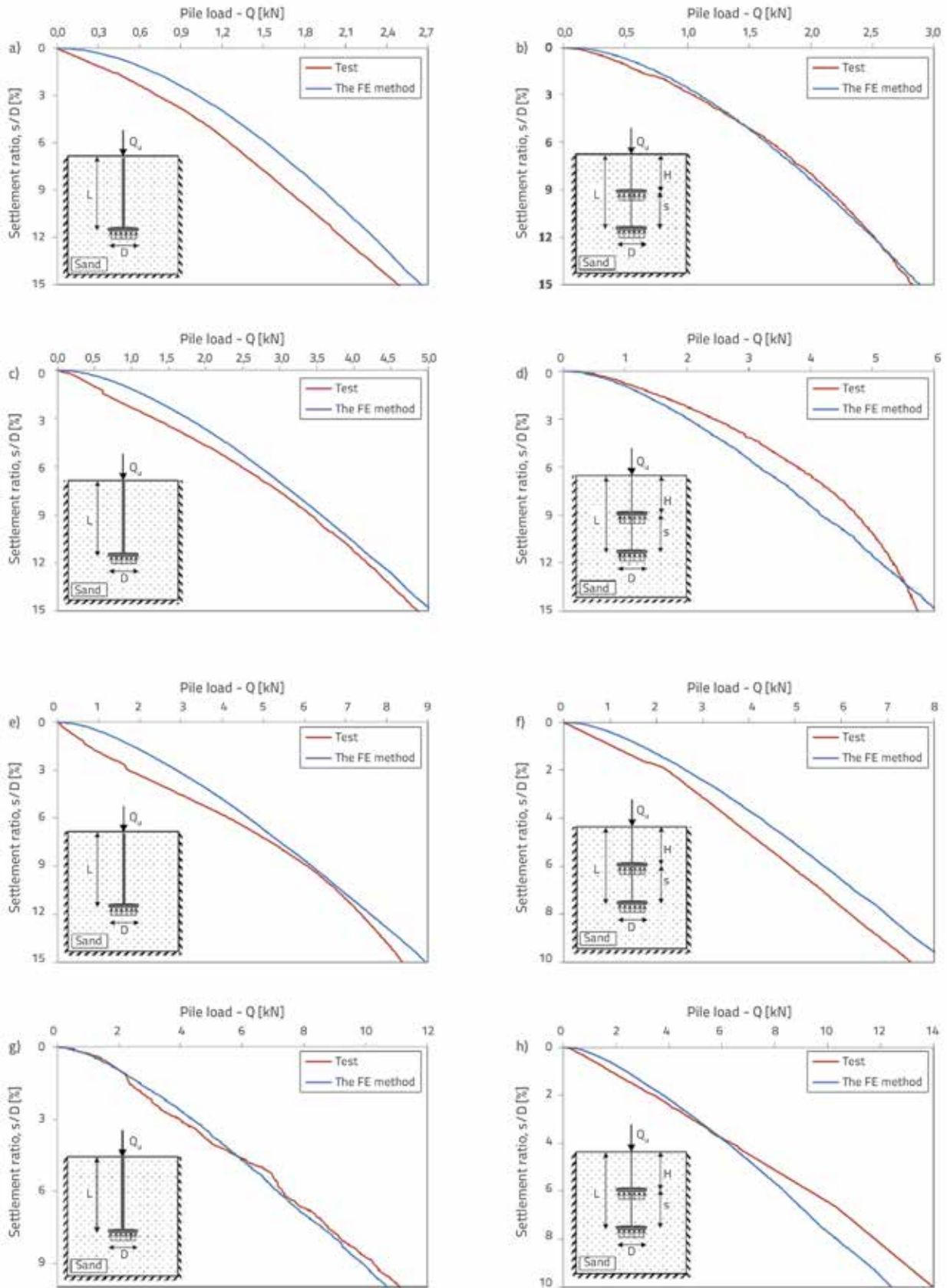


Figure 10. Comparison of test and numerical results for different helical plate diameter: a) HP-1 test; b) HP-2 test; c) HP-7 test; d) HP-8 test; e) HP-13 test; f) HP-14 test; g) HP-19 test; h) HP-20 test

It is also user-friendly and suitable for practical applications. A total of five parameters are accepted as inputs, namely; dilatancy angle (Ψ), soil plasticity (ϕ and c), and soil elasticity (E and ν). In this model, the "first-order" approach is used to define the soil behaviour. It is clear from the literature that drained soil conditions are assumed in the analysis of sand soil. Model parameters representing sand soil are given in Table 6: In this table, the parameters were obtained from classical soil mechanics tests, except for the angle of dilatancy, Ψ , which is assumed to be 8° , ($\phi-30^\circ$) [21]. The helical pile shaft is modelled according to the elastic linear model. The helical pile shaft values were assumed as Poisson's ratio and Young's modulus values of 0.3 and $200 \cdot 10^6$ kPa, respectively.

Table 5. Soil parameters in Mohr-Coulomb model

Parameter	Value
Unit weight, γ_n [kN/m ³]	15.84
Loading stiffness, E_u [kPa]	15000
Cohesion, c [kPa]	0.3
Internal friction angle, ϕ [°]	38
Angle of dilatancy, Ψ [°] ($\phi-30^\circ$)	8
Poisson's ratio, ν	0.2

In this part of the study, the validity of numerical model is determined via comparison of numerical simulations and test results. For this purpose, a series of numerical analyses were conducted on the helical pile plates at different numbers (single and double plate) and diameters ($D = 50, 75, 100$ and 125 mm) to define compression behaviour of helical piles placed in sandy soil. The load (Q)-settlement ratio (s/D) curves, obtained for both numerical and model tests for different helical plate diameters (D), are presented in Figure 10 as graphics. The comparison of numerical and test results shows that results for different helical plate diameters and numbers are compatible. Test and numerical results are compared for each diameter. $s/D = 0$ and $s/D = 1$ configurations are given as examples in Figure 10. In addition, ultimate loads obtained from numerical analyses are presented in Table 7, together with model test results for 5 %D of failure criteria. Compatible test and numerical results were obtained for different helical plate diameters and numbers. As known, the main purpose of numerical analyses is to reduce the design cost and design time. This consistency in test and numerical analysis results can provide cost and time savings in helical pile design. For this decision, it is important to correctly determine geotechnical properties of soil environment. Figure 11 presents vertical displacement contours and compressive failure mechanisms corresponding to vertical displacements of 5 mm (5 %D) from the top of helical piles.

Table 6. Comparison of test and numerical analyses

Pile No.	No. of helixes	D (helix diameter) [mm]	s/D	Measured capacity [kN]	
				Test (5%D)	FE analysis (5%D)
HP-1	Single	50	0	1.15	1.25
HP-2	Double		1	1.40	1.42
HP-3	Double		1.5	1.73	1.48
HP-4	Double		2	2.10	1.51
HP-5	Double		2.5	2.15	1.58
HP-6	Double		3	1.90	1.61
HP-7	Single	75	0	2.15	2.42
HP-8	Double		1	3.35	2.83
HP-9	Double		1.5	3.80	2.98
HP-10	Double		2	4.90	3.08
HP-11	Double		2.5	5.00	3.20
HP-12	Double		3	4.20	3.27
HP-13	Single	100	0	3.15	4.26
HP-14	Double		1	4.25	4.96
HP-15	Double		1.5	4.65	5.27
HP-16	Double		2	5.60	5.47
HP-17	Double		2.5	6.30	5.68
HP-18	Double		3	5.30	5.88
HP-19	Single	125	0	6.60	6.80
HP-20	Double		1	7.83	8.10
HP-21	Double		1.5	8.10	8.60
HP-22	Double		2	10.53	9.10
HP-23	Double		2.5	10.14	9.34
HP-24	Double		3	9.20	9.65

Helical pile type HP100 for different s/D ratios is given here as an example. When these demonstrations are examined (by focusing on the spacing between helix plates), it can be seen that the individual bearing failure mechanism is observed in case of $s/D \geq 1.5$. These findings confirm the data obtained by model testing.

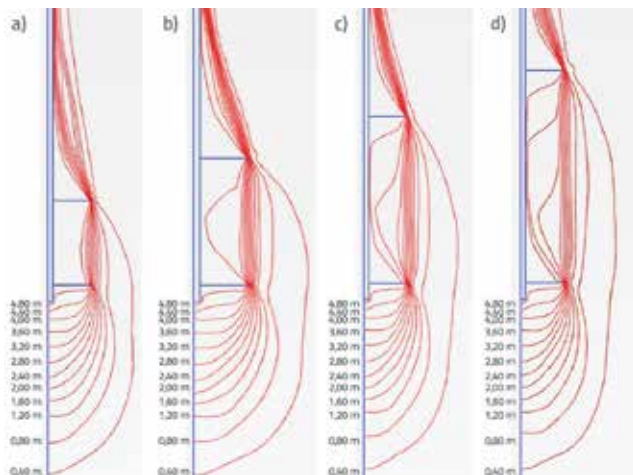


Figure 11. Settlement contours with different s/D ratios for 5 mm (5 %D) top displacement for HP100 type piles: a) $s/D = 1.0$; b) $s/D = 1.5$; c) $s/D = 2.0$; d) $s/D = 2.5$

7. Conclusion

A series of laboratory model tests and numerical analyses, including theoretical approaches for axially compressive loaded single helical piles in sand soil, are presented in this research. The helical plate number, helical plate diameter, and helical plate spacing, were selected as variables to determine the compressive behaviour. Load-settlement curves obtained

from the experimental and numerical studies are presented in detail. The findings can be listed as follows:

- Despite a relatively small size and cross-section, model helical piles were successfully placed on the sand soil.
- The load–settlement characteristics of model helical piles subjected to compression reveal typical trends, i.e. the first segment exhibits linear behaviour and the remaining one exhibits a highly nonlinear and then near-linear behaviour.
- Double helix piles showed up to about two times greater resistance compared to single-helix piles.
- Although helical diameter increased linearly, the increase in compressive load is nonlinear. The compressive load increases by up to about three times while the helical diameter doubled.
- Three different failure mechanisms (5 %D, 10 %D and Davisson's criterion method) were defined for estimating the ultimate compressive load. The best fits were obtained in 5 %D method, and so this method was used to interpret the results.
- Harmonious trends were observed between the numerical and model test results. The finite element demonstrations indicate that the individual bearing failure mechanism is observed in case of $s/D \geq 1.5$.
- The soil environment and helical pile behaviour under compressive loadings can be successfully simulated with the Mohr Coulomb model, where model parameters can easily be determined by conventional geotechnical laboratory tests.
- The results of this study show that, with an accurate geotechnical data set, helical pile design can be performed rapidly and more economically.
- The results of this study serve as an alternative to the modelling of the compressive behaviour of the helical piles that are becoming increasingly popular in geotechnical engineering applications.

REFERENCES

- [1] Tsuha, C.H.C., Aoki, N., Rault, G., Thorel, L., Garnier, J.: Evaluation of the efficiencies of helical anchor plates in sand by centrifuge model tests, *Canadian Geotechnical Journal*, 49 (2012), pp.1102–1114, <https://doi.org/10.1139/T2012-064>.
- [2] Nazir, R., Chuan, H.S., Niroumand, H., Kassim, K.A.: Performance of single vertical helical anchor embedded in dry sand, *Measurement*, 49 (2013) 1, pp. 42–51, <https://doi.org/10.1016/j.measurement.2013.11.031>.
- [3] Sakr, M.A., Nazir, A.K., Azzam, W.R., Sallam, A.F.: Behaviour of grouted single screw piles under inclined tensile loads in sand, *Electronic Journal of Geotechnical Engineering*, 21 (2016), pp. 571–592
- [4] Livneh, B., Naggar, M.H.M.: Axial testing and numerical modelling of square shaft helical piles under compressive and tensile loading, *Canadian Geotechnical Journal*, 45 (2008) 8, pp. 1142–1155, DOI: 10.1139/T08-044.
- [5] Sakr, M.: Installation and performance characteristics of high capacity helical piles in cohesionless soils, *The Journal of the Deep Foundations Institute*, 5 (2011) 1, pp. 39–57, <https://doi.org/10.1179/dfi.2011.004>.
- [6] Malik, A.A., Kuwano, J., Tachibana, S., Maejima, T.: End bearing capacity comparison of screw pile with straight pipe pile under similar ground conditions, *Acta Geotechnica*, 12 (2017) 9, pp. 415–428
- [7] Li, W., Deng, L.: Axial load tests and numerical modelling of single-helix piles in cohesive and cohesionless soils, *Acta Geotechnica*, 2018, <https://doi.org/10.1007/s11440-018-0669-y>.
- [8] Sprince, A., Pakrastinsh, L.: Helical pile behaviour and load transfer mechanism in different soils, 10th International Conference on Modern Building Materials, Structures and Techniques, pp.1174–1180, 2010.
- [9] Salhi, L., Nait-Rabah, Q., Christophe, D., Roos, C.: Numerical modelling of single helical pile behaviour under compressive loading in sand, *Electronic Journal of Geotechnical Engineering*, 18 (2013), pp. 4319–4338.

- [10] Polishchuk, A.I., Maksimov, F.A.: Numerical analysis of helical pile–soil interaction under compressive loads, IOP Conference Series: Materials Science and Engineering, 262 (2017), pp. 1-8, <https://doi.org/10.1088/1757-899X/262/1/012099>.
- [11] Mohajeranin, A., Bosnjak, D., Bromwich, D.: Analysis and design methods of screw piles, Soils and Foundations, 56 (2016) 1, pp. 115-128, <https://doi.org/10.1016/j.sandf.2016.01.009>.
- [12] Mitsch, M.P., Clemence, S.P.: The uplift capacity of helix anchors in sand, Uplift behaviour of anchor foundations in soil, American Society of Civil Engineers, New York, pp. 26–47, 1985.
- [13] Zhang, D.J.Y., Chalaturnyk, R., Robertson, P.K., Segoo, D.C., Cyre, G.: Screw anchor test program (Part I & II): instrumentation, site characterization and installation, Proceedings of the 51st Canadian Geotechnical Conference, Edmonton, 1998.
- [14] Sakr, M.: Lateral resistance of helical piles in oil sands, International Foundation Congress and Equipment Expo Contemporary Topics in Deep Foundations, pp. 464-471, [https://doi.org/10.1061/41021\(335\)58](https://doi.org/10.1061/41021(335)58), 2009.
- [15] Elsherbiny, Z.H., Naggar, M.H.: Axial compressive capacity of helical piles from field tests and numerical study, Canadian Geotechnical Journal, 50 (2013), pp. 1191–1203, <https://doi.org/10.1139/cgj-2012-0487>.
- [16] Meyerhof, G.G., Adams, J.I.: The ultimate uplift capacity of foundations, Canadian Geotechnical Journal, 5 (1968) 4, pp. 225–244, [https://doi.org/10.1061/\(ASCE\)GT.1943-5606.0000478](https://doi.org/10.1061/(ASCE)GT.1943-5606.0000478).
- [17] Vesic, A.S.: Breakout resistance of objects embedded in ocean bottom, Journal of the Soil Mechanics and Foundations Division, ASCE, 97 (1971) 9, pp. 1183-1205
- [18] Canadian Geotechnical Society: Canadian Foundation Engineering Manual, 4th Edition, pp. 488, 2006.
- [19] Plaxis 2D: Material Models Manual, Geotechnical Finite Element Software, Delft, Netherlands, 2018.
- [20] Brinkgreve, R.B.J., Broere, W., Waterman, D.: Plaxis finite element code for soil and rock analysis, 2D–Version 8.6, 2004.
- [21] Bolton, M.D.: The strength and dilatancy of sands, Géotechnique, 36 (1986) 1, pp. 65-78, <https://doi.org/10.1680/geot.1986.36.1.65>.
- [22] Davisson, M.T.: High capacity piles, Proceedings of Lecture Series of Innovations in Foundation Construction, ASCE, Illinois section, Chicago, pp. 81–112, 1972.
- [23] Butler, H.D., Hoy, H.E.: The Texas quick-load method for foundation load testing, User's manual, Rep. No. FHWA-IP-77–8., Texas State Department of Highways and Public Transportation, Austin, Texas, 1977.
- [24] ISSMFE: Axial pile loading test – Part I: Static loading, Geotechnical Testing Journal ASTM, 8 (1985) 2, pp. 79–80, <https://doi.org/10.1520/GTJ10514J>.
- [25] Reese, L.C., O'Neill, M.W.: Drilled shafts: construction procedures and design methods, FHWA-HI-88–042, Federal Highway Administration, McLean, 1988.
- [26] FDOT: Standard specifications for road and bridge construction, Florida Department of Transportation (FDOT), 1999.
- [27] Terzaghi, K.: Discussion of the progress report of the committee on the bearing value of pile foundations, Proceedings of the American Society of Civil Engineers, 68 (1942), pp. 311–323
- [28] O'Neill, M.W., Reese, L.C.: Drilled shafts: Construction procedures and design methods, Publication No. FHWA-IF-99–025, Office of Infrastructure, Federal Highway Administration, Washington, D.C., 1999.